Journal of Hydrology 521 (2015) 18–33

Contents lists available at ScienceDirect

Journal of Hydrology

journal homepage: www.elsevier.com/locate/jhydrol

Climate change and water resources management in the Upper Santa Cruz River, Arizona

Eylon Shamir [a,*], Sharon B. Megdal [b], Carlos Carrillo [c], Christopher L. Castro [c], Hsin-I Chang [c], Karletta Chief [e], Frank E. Corkhill [d], Susanna Eden [b], Konstantine P. Georgakakos [a,f], Keith M. Nelson [d], Jacob Prietto [b]

[a] Hydrologic Research Center, San Diego, CA, United States
[b] Water Resources Research Center, The University of Arizona, Tucson, AZ, United States
[c] Atmospheric Science Department, The University of Arizona, Tucson, AZ, United States
[d] Arizona Department of Water Resources, Phoenix, AZ, United States
[e] Soil, Water and Environmental Sciences, The University of Arizona, Tucson, AZ, United States
[f] Scripps Institution of Oceanography, University of California, San Diego, United States

ARTICLE INFO

Article history:
Received 8 September 2014
Received in revised form 21 November 2014
Accepted 22 November 2014
Available online 29 November 2014
This manuscript was handled by Geoff Syme, Editor-in-Chief, with the assistance of Konstantine P. Georgakakos, Associate Editor

Keywords:
Rainfall generator
Santa Cruz River
Ephemeral streams
Water resources management
Climate change

SUMMARY

Episodic streamflow events in the Upper Santa Cruz River recharge a shallow alluvial aquifer that is an essential water resource for the surrounding communities. The complex natural variability of the rainfall-driven streamflow events introduces a water resources management challenge for the region. In this study, we assessed the impact of projected climate change on regional water resources management. We analyzed climate change projections of precipitation for the Upper Santa Cruz River from eight dynamically downscaled Global Circulation Models (GCMs). Our analysis indicates an increase (decrease) in the frequency of occurrence of dry (wet) summers. The winter rainfall projections indicate an increased frequency of both dry and wet winter seasons, which implies lower chance for medium-precipitation winters. The climate analysis results were also compared with resampled coarse GCMs and bias adjusted and statistically downscaled CMIP3 and CMIP5 projections readily available for the contiguous U.S. The impact of the projected climatic change was assessed through a water resources management case study. The hydrologic framework utilized includes a rainfall generator of likely scenarios and a series of hydrologic models that estimate the groundwater recharge and the change in groundwater storage. We conclude that climatic change projections increase the uncertainty and further exacerbate the already complicated water resources management task. The ability to attain an annual water supply goal, the accrued annual water deficit and the potential for replenishment of the aquifer depend considerably on the selected management regime.

1. Introduction

Meeting water demands in semi-arid and arid regions is a particularly challenging task in communities that rely on local water resources and who also lack the infrastructure for multi-year storage. Precipitation variability in these regions often consists of long dry spells with episodic wet events that replenish their reservoirs. This study focuses on the Upper Santa Cruz River (USCR) north of the border shared by Arizona in the United States (U.S.) and Sonora, Mexico (Fig. 1). In this region, the city of Nogales, Arizona and surrounding water users extract their water supply from a relatively shallow and small alluvial aquifer beneath the ephemeral channel of the USCR (Erwin, 2007). The main source of recharge to this aquifer is the highly variable intermittent rainfall-driven streamflow events on the USCR (Erwin, 2007), which implies that the natural variability of the river flow and the groundwater recharge are tightly linked (Liu et al., 2012; Nelson, 2010; Shamir et al., 2007a,b).

In this study, we demonstrate the usability of a hydrological modeling framework for decision making regarding groundwater pumping and addressing regional statutory management goals as applied to arid and semi-arid area. The modeling framework, based on the approach of Shamir et al. (2005, 2007a), was enhanced in this work to enable impact assessment of projected future rainfall scenarios, as interpreted from dynamically downscaled regional

* Corresponding author.
E-mail address: eshamir@hrcwater.org (E. Shamir).

http://dx.doi.org/10.1016/j.jhydrol.2014.11.062
0022-1694/

climate models. In the core of the modeling framework there is a weather generator that produces synthetic likely rainfall realizations. These realizations are used as input to simulate streamflow, channel routing, groundwater recharge and groundwater levels and to assess the impact of projected future changes in precipitation under different groundwater management scenarios.

An extensive stakeholder involvement process was deployed to inform the technical modeling. Stakeholders were engaged to raise water management issues and provide feedback and comments on the hydrologic modeling framework. Reliability of water supply and impacts of over pumping on groundwater levels and riparian corridors were identified as their most significant concerns.

To date, studies of future climate analysis that include in their domain the study area were mainly focused on broad regional and seasonal perspectives and extreme events (review is provided in Section 3). As demonstrated in Section 1.1, the wide regional perspective is often inadequate for describing the hydrologic response in the area studied herein. In the study area that represents many other semiarid and arid ephemeral environments, it is the high spatiotemporal resolution and the detailed characteristics of the rainfall that dominate the intermittent streamflow and groundwater recharge events. In this study we address this information gap and present a modeling framework that connects the future climate projections to the scale that is needed for a meaningful hydrologic impact assessment.

Perhaps the most important contribution of the present study is the detailed analysis of the important contributors that provide useful management information for arid and semi-arid regions, when it is necessary to incorporate climatic variability and change on small scales. The details of such analysis are very different from approaches that have focused on wetter regions (e.g., Georgakakos et al., 2012) whereby long term averages dominate water management decisions and where intermittence of management-significant events maintains a more or less uniform distribution throughout the records.

In the remainder of this section we discuss the approach followed for the hydrologic impact assessment. In Section 2 we describe the study area and its observed climate influences. In Section 3 we present a discussion of climate projections of future rainfall for the study area from the results of analysis of eight carefully selected dynamically downscaled regional climate models. In addition, we compare the results of the eight downscaled models to CMIP3 and CMIP5 readily available projections of coarse GCMs and statistically downscaled GCMs. In Section 4 we describe the hydrologic modeling framework and the incorporation of the climate projection results into the framework. A water resources

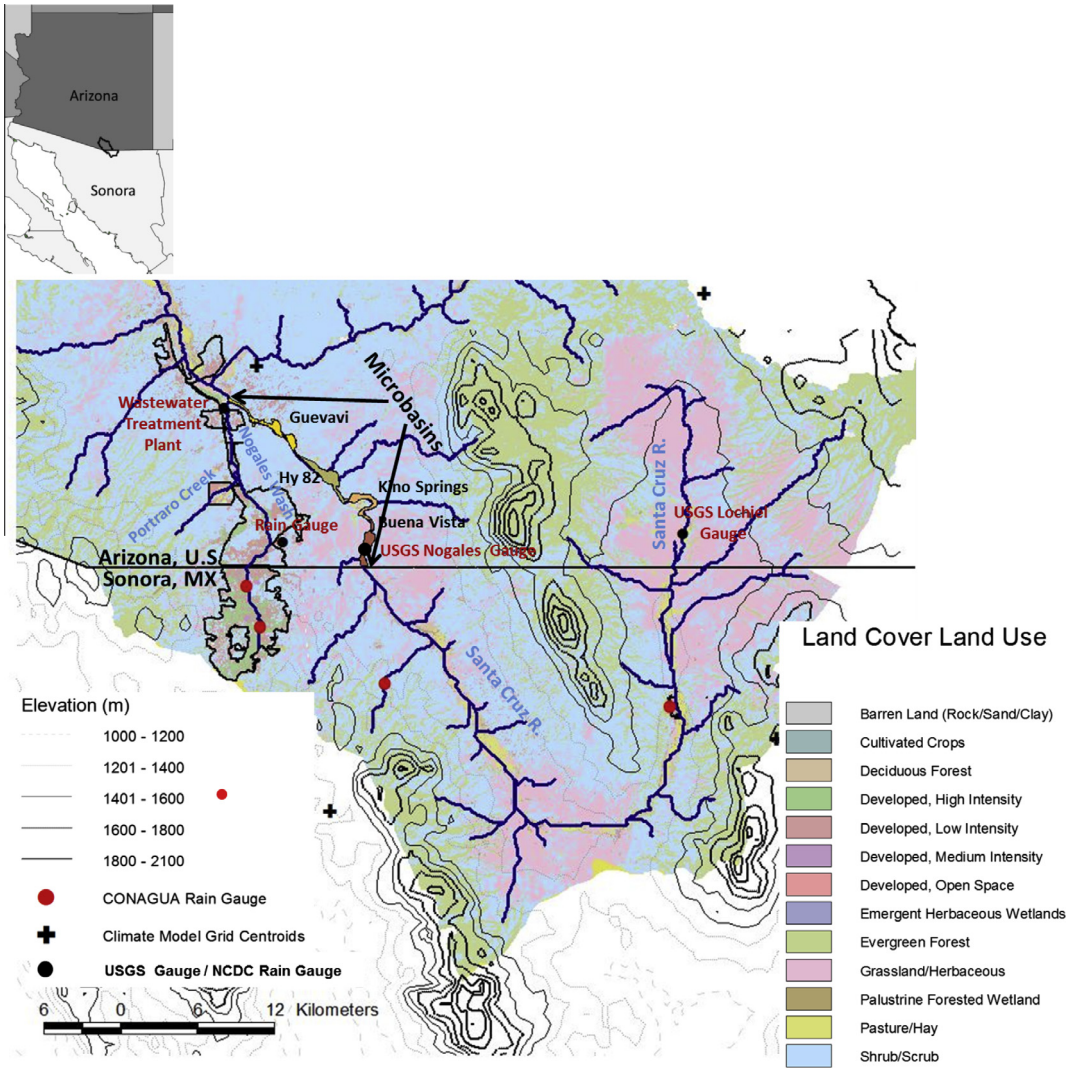

Fig. 1. Map of the study region.

management case study is presented and the climate implications for management decision making are explored via discussion of the case study's results in Sections 5 and 6.

1.1. Hydrologic impact assessment approach

In order to generate GCM rainfall projections that are adequate to serve as forcing for catchment scale hydrologic models, dynamical and statistical downscaling methods were developed (e.g. Wilby and Wigley, 1997). Dynamical downscaling methods use GCM variables as boundary conditions to drive a nested Regional Circulation Model with higher spatial and temporal resolution that simulates regional climate processes and orographic influences. While the dynamically downscaled approach provides highly resolved and physically based information (spatial and temporal) for a range of congruent atmospheric variables, it requires considerable computational resources and often yields a single downscaled realization. In addition, the simulated variables often require additional bias adjustment for the downscaled high-resolution fields and/or for the resultant streamflow (Georgakakos et al., 2012).

Statistical downscaling methods for GCM variables provide an attractive and less computational intensive alternative. These methods depend on statistical associations between local observed records (e.g., temperature or rainfall) and atmospheric variables simulated by the GCMs (e.g., sea level pressure, specific humidity) and often assume constancy of these statistical associations in the future. Many recent studies conducted in the U.S. for assessment of future climate impact on the hydrologic regime and water resources have been using the statistical downscaled projections provided by the U.S. Bureau of Reclamation (Reclamation, 2011).

Although simple and efficient to apply, statistical downscaling projections may have shortcomings when used in relatively small basins located in arid and semi-arid regions. In these regions, the flows in the often ephemeral channels are dependent on the nuanced characteristics of the episodic rainfall events (e.g. daily, hourly). Thus there is need for a hydrologic assessment approach that explicitly considers the high-resolution temporal features of rainfall as these are critical for the representation of hydrologic regimes.

By way of demonstration, consider the cumulative distribution of daily precipitation rainfall (days with rainfall greater than 0.2 mm/day) of the historic period (1955–2010) for the study area shown for several cases in Fig. 2. The black lines represent 134 bias adjusted and statistically downscaled simulations of selected representative CMIP5 climate models with various green-house gas emission scenarios for the grid cell that includes the Upper Santa Cruz River at the U.S.–Mexico border crossing (Reclamation, 2011).

The red line is the historical gridded product at 1/8° that was used as a reference for the adjustment of the climate model projections (Maurer et al., 2002), and the blue line represents the cumulative distribution of the observed rainfall at the Nogales gauge (Fig. 1). The three panels show the cumulative distribution of the temporal mean (upper panel), temporal standard deviation (middle panel), and number of occurrences (lower panel) of the daily rainfall time series.

For the study area, the statistically downscaled gridded projections capture reasonably well the distribution of the historical gridded mean daily rainfall values (upper panel Fig. 2). The distribution of means is also in accordance to that of the point measurements at the Nogales gauge. However, the statistical downscaling results underestimate the variability of the daily rainfall (middle panel), and substantially overestimates the number of daily rainfall events (lower panel). The differences between the historical gridded daily rainfall and the gauge daily rainfall indicative of a convective regime in a semi-arid region are also displayed in Fig. 2.

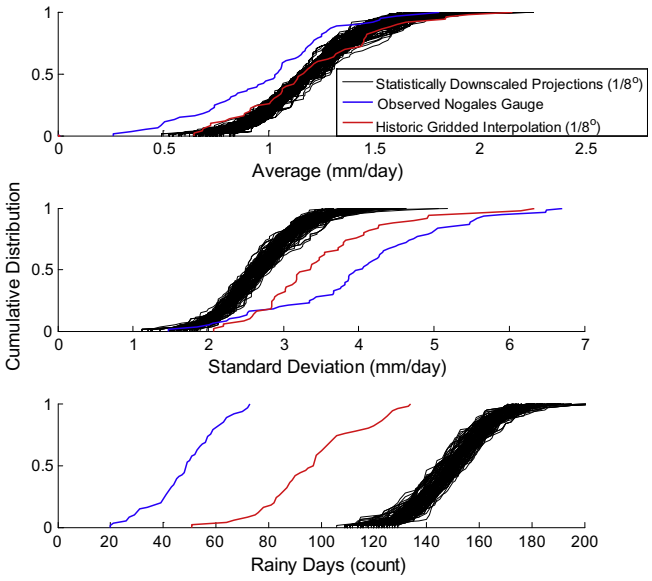

Fig. 2. Cumulative distribution of rainfall time series (1955–2010) for the means, standard variations and number of rainy days (upper, middle, and lower panel, respectively). The black lines are 134 realizations of bias adjusted and statistically downscaled to 1/8° time series of CMIP5 available from Reclamation (2011), the red line is the historical interpolated gridded observed daily product and the blue line represents the observed daily rainfall from the gauge site at Nogales. (For interpretation of the references to color in this figure legend, the reader is referred to the web version of this article.)

The gauge data has a lower average, higher standard deviation and markedly fewer occurrences of daily rainfall events.

In this study we address the need for high temporal resolution by using a modeling framework that is based on a rainfall generator that simulates ensembles of likely scenarios that represent the statistical characteristics of the observed gauge records. Rainfall generators have been used in climate impact studies to represent the rainfall characteristics at the spatiotemporal scale that is relevant for the hydrologic regime of the specific region (e.g., Peleg and Morin, 2014; Peleg et al., in preparation; Paschalis et al., 2013).

The climate projection analysis is focused on identifying differences between the historic and projected periods that can guide modifications in the rainfall generator for application in projected future climatic periods. The assumption guiding this approach is that the rainfall generation model structure (and not necessarily the parameters) remains the same for the past and the future climates in this semi-arid region. The general nature of the model structure (discussed in a later section) renders this assumption reasonable.

An advantage of our proposed modeling framework that involves a stochastic rainfall generator that produces ensembles of likely-to-occur rainfall realizations is that the probabilistic representation of the rainfall by the ensembles embodies the uncertainty associated with the natural variability (Wilks and Wilby, 1999). For water resources management, and based on feedback from the stakeholders, the proposed modeling approach addresses their need to account for the consequences of various management decisions in probabilistic terms.

2. Study area

The Santa Cruz River is an ephemeral tributary in Southern Arizona that drains into the Gila River, a branch of the Colorado River (Fig. 1). The drainage area at the USGS Nogales streamflow gauge (USGS # 09480500), about 10 km east of the city of Nogales, Arizona, is about 1400 km^2, of which approximately 1150 km^2 are in

Mexico. From its headwaters in the San Rafael Valley in Southern Arizona, the river flows southward into Mexico and bends northwards towards Arizona to re-cross the international border. The river length in Mexico is about 60 km and includes short sections with perennial flow. The drainage area is sparsely populated and its landscape comprises heavily grazed desert scrub with deciduous broad leaf forest in the higher elevations. Downstream of the USGS Nogales gauge in the vicinity of the border crossing there is a series of four relatively small shallow alluvial aquifers (microbasins) bounded by the low permeability Nogales Formation. The microbasins are separated from each other by outcrops of the less permeable Nogales formation and/or shallow bedrock that limit the hydraulic connection between them (Halpenny and Halpenny, 1988).

The younger alluvium in the four microbasins is a highly productive geologic formation with transmissivity values ranging from 400 to 2800 $m^2\ d^{-1}$ (Erwin, 2007). The thickness of the younger alluvium in the microbasins ranges 10–40 m (Erwin, 2007).

Recent and yet unpublished modeling results, geophysical studies, and exploration borings indicate the existence of deep underflow zone beneath the microbasins. It was seen, for instance, that during long periods of no-streamflow recharge, the water levels in the microbasins dropped considerably. This underflow from the microbasins is estimated at about 4000–6000 ac-ft yr^{-1} (~5–7.5 Mm^3 [million cubic meter] yr^{-1}). In addition, it was recently estimated that about 6000–7000 ac-ft yr^{-1} (~7.5–8.6 $Mm^3\ yr^{-1}$) of groundwater flow north from the Guevavi microbasin to the downstream aquifer. This is likely a larger amount than the receiving underflow that crosses from Mexico to the Buena Vista microbasin (Fig. 1). The water loss of the microbasins compounds the impact of drought on water resources management in this region.

The region has two wet seasons: summer (July–September), and winter (November–March). Spring (April–June) is mostly dry and fall (October) is dry with rare intense rainfall events. These fall events are capable of producing large storms over Southern Arizona instigated by remnants of tropical cyclonic storms over the Pacific Ocean. The summer storms are mainly driven by isolated convective cells that produce intense short-lived rainfall events. Winter storms originate almost entirely from large scale low pressure frontal systems approaching from the west and southwest. These storms may last for a few days, with persistent rain over large areas (Hirschboeck, 1985). The different seasonal storm characteristics yield different streamflow responses in the river channel. The winter storms yield a relatively slow rising hydrograph limb and long lasting baseflow, while the summer flow commonly appears as a sharp rising hydrograph limb followed by a relatively short period of baseflow (e.g. Shamir et al., 2007a).

The nature of the hydrologic variability in the region is well demonstrated in Fig. 3 where the summer (red) and winter (black) are shown for streamflow and precipitation in the upper and lower panels, respectively. The gauge streamflow and precipitation records show that both wet seasons (i.e., summer and winter) exhibit large inter-annual variability. The straight lines in these figures indicate the arithmetic seasonal averages. The averages of streamflow for winter and for summer are almost equal (~10 Million m^3 - yr^{-1}). However, because of the large inter-annual variability, knowledge of these arithmetic averages has little value for projecting flow and thus for water resources management.

The figure shows that only 23% and 33% of the winters were above average for streamflow and rainfall, respectively. Summers have higher frequencies of years with higher than the average, 36% and 43%, streamflow and rainfall, respectively. This positively skewed characteristic implies that most years are relatively dry, and only infrequent wet seasons are contributing to the relatively high average values.

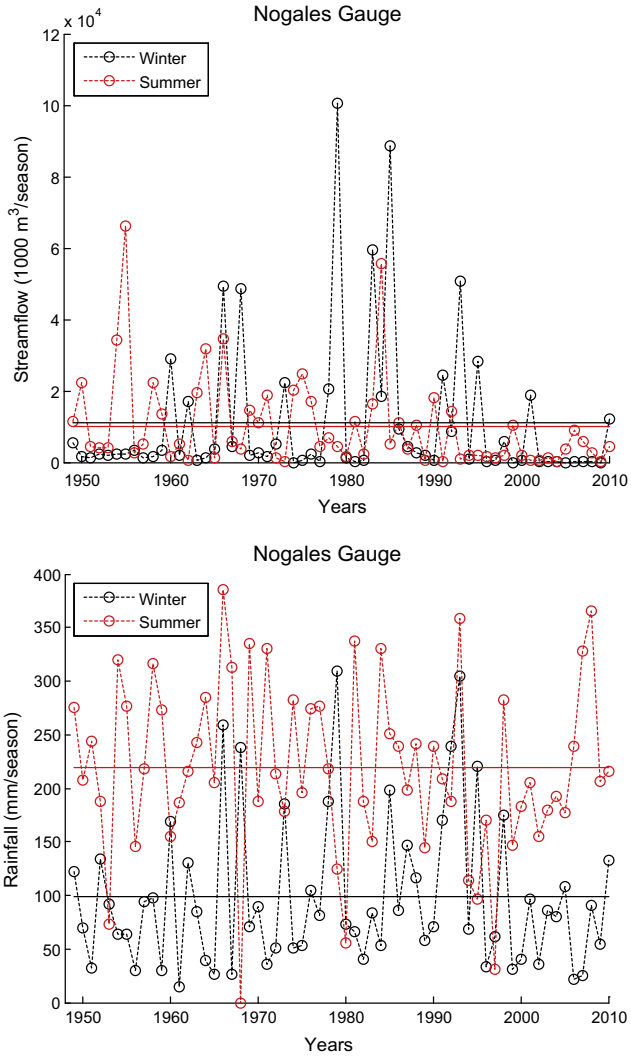

Fig. 3. Summer (red) and winter (black) seasonal streamflow volume (upper panel) and total seasonal rainfall (lower panel) time series in the Nogales area. Straight lines indicate the arithmetic inter-annual averages. (For interpretation of the references to color in this figure legend, the reader is referred to the web version of this article.)

In addition, there are long multi-year sequences in which winter and summer were dryer than the average in terms of streamflow. For example, during 1948–1959 and 1996–2010 (excluding 2001, which was slightly above average) there were long sequences of winters that were dryer than average. A long spell of dryer than average summers was recorded in 1993–2010, except for 1999, which was slightly above average.

Although winters and summers have almost the same average streamflow, the average summer rainfall is more than twice the average winter rainfall (220 mm versus 100 mm, respectively). This difference between the seasonal rainfall and streamflow is attributed to the distinctive seasonal characteristics of rainfall spatial and temporal variability and its impact in streamflow generation (Shamir et al., 2007a; Morin et al., 2005).

The study area is within the Santa Cruz Active Management Area (SCAMA), one of five regions established under the Arizona Groundwater Management Act (GMA), where a water management and policy framework was implemented to control severe overdraft of groundwater, provide effective allocation of groundwater resources, and improve groundwater management through water planning, conservation, and augmentation. The SCAMA has

a dual statutory water management goal: "to maintain a safe-yield condition in the active management area and to prevent local water tables from experiencing long term declines." The term safe yield is defined in the statute as a "water management goal which attempts to achieve and thereafter maintain a long-term balance between the annual amount of groundwater withdrawn in an AMA and the annual amount of natural and artificial recharge in an AMA." The Arizona Department of Water Resources (ADWR) is the regulatory agency that implements groundwater management law. Water users within AMAs are required to adhere to applicable rules for conservation and water use. These include AMA specific Assured Water Supply (AWS) rules that require long-term water resource planning for water providers serving newly developed or growing areas.

Water providers must prove they have available supplies for 100 years, and their plans must be compatible with AMA goals. The SCAMA's AWS rules are in draft form pending an end to the statewide gubernatorial moratorium on rulemaking. Although the statute does not explicitly mention conjunctive management of surface water and groundwater, as discussed above, the major source of groundwater recharge in the SCAMA consists of the intermittent streamflow events in the river channel of the Santa Cruz River (e.g. Erwin, 2007; Nelson, 2007). Therefore, surface flows must be considered for any long-term groundwater management plan.

Several studies in recent years reported changes in the hydrologic regime of the USCR region during recent historical climate: reduction in summer streamflow volume and number of summer streamflow occurrences (Thomas and Pool, 2006; Shamir et al., 2007b); reduction in the duration of baseflow (Nelson, 2010); reduction in number of summer precipitation events but no indication for a change in total rainfall (Shamir et al., 2007b); and a substantial increase in the monthly variability of streamflow since the 1970s (e.g. Shamir et al., 2007b). These changes in the hydrologic regime, as well as future climate projections for the region, which are further elaborated in Section 3, introduce compounding management challenges for the region's water resources.

3. Climate change projections

Because groundwater recharge occurs during relatively short intermittent streamflow events and the aquifer is partially isolated from evaporation and transpiration fluxes, the hydrologic impact of future projected warming on the microbasins is still an unanswered question (Garfin et al., 2013). Future climate projections of precipitation in the study region must consider the winter and summer precipitation seasons separately. The recent report, Assessment of Climate Change in the Southwest United States (Garfin et al., 2013), projected increased probability of drier winters attributed to the projected widening with time of the high pressure subtropical Hadley cell, which in turn will push the jet stream, the moisture carrier for the regional winter storms, northward. The summer convective rainfall is a more challenging phenomenon to predict because its origin, frequency, and distribution are not as tightly linked to larger scale meteorological synoptic conditions. In addition, the southwestern monsoonal convective storms are relatively small scale phenomena compared to the scale that is resolved by the current global climate models.

The inter-annual frequency and spatial pattern of the monsoon, however, is found to be related to the latitudinal shift in the mid-level subtropical ridge over the southwestern U.S. (i.e. its northern displacement yields wetter summers). Thus, large scale climatological features observed in GCM simulations can be used as teleconnection indicators for summer precipitation in the study region. The location of this ridge is tied to different phases of the Pacific Northern America tele-connection pattern (Carleton et al., 1990). Recent studies indicated that the North American Monsoon inter-annual variability is related to the El Niño Southern Oscillation (ENSO) and Pacific Decadal Variability (PDO) forced atmospheric teleconnection patterns emanating from the tropical Pacific (e.g. Castro et al., 2007b) and/or antecedent land surface conditions (e.g. Grantz et al., 2007). This relationship implies that during years with anomalously high sea surface temperature in the Eastern Pacific the North American Monsoon season is delayed and shortened (Seth et al., 2011; Cook and Seager, 2013). Castro et al. (2007a,b) also found a long-term increase in the late twentieth century (1950–2002) of the diurnal cycle strength of summer convection, which implies intensification of thunderstorms.

3.1. Analyses of the regional downscaled models

Regional Climate Model (RCM) dynamically downscaled precipitation projections for the study domain [31–31.5°N, 111.5–110.44°W] were obtained from the University of Arizona Atmospheric Sciences Department (UA-ATMO) and the North American Regional Climate Change Assessment Program (NARCCAP). These RCMs were forced by Global Circulation Models (GCM) simulations using the A2 green-house gas emissions scenario [Intergovernmental Panel on Climate Change (IPCC) Special Report on Emission Scenarios] for the 21st century. The A2 emissions scenario projects slow economic growth and an ever-growing global population.

Because of the large spatial and temporal variability in the Southwest, it is imperative to select GCMs that simulate reasonably well the dominant climatic processes for the region. The GCMs should at least reproduce the region's climatology and inter-annual variability of the large-scale atmospheric circulation. It is also important to select GCMs that simulate the mesoscale synoptic conditions of the monsoon ridge and Pacific-SST forced tele-connection that modulate its positioning in the early part of the summer. In addition, it is essential to simulate the mesoscale conditions that modulate the diurnal convective summer precipitation (Castro et al., 2012).

The UA-ATMO applied the Advanced Research version (ARW) of the Weather Research and Forecasting (WRF) Model (Version 3.1) to downscale two well-performing coupled models from the Inter-comparison Project Phase 3 (CMIP3) IPCC Assessment Report 4 (AR4) GCMs (Dominguez et al., 2010). These selected GCMs are the HADCM3 by the Hadley Centre for Climate Prediction and Research at the Meteorological Office in United Kingdom; and the MPI-ECHAM5 from the European Center for Medium-Range Weather Forecast (ECMWF) and the Max Planck Institute. These two GCMs were selected out of 24 IPCC CMIP3 competing models for their ability to (1) represent the observed temperature and precipitation climatologies, and (2) simulate the large-scale circulation features that drive moisture fluxes into the Southwestern U.S. (Dominguez et al., 2010). The winter ENSO variability that affects the location of the subtropical jet stream and consequently winter rain in the Southwest was evaluated by looking at the model simulations of the 250 mbar geopotential height field (GPH). The skill of these two selected models to resolve observed warm-dry and cool-wet tele-connection patterns over the Pacific Northwest and Southwest U.S. associated with El Nino and La Nina events was also confirmed by Zhang et al. (2012).

The UA-ATMO ARW-WRF downscaled simulations (hereinafter WRF-HAD and WRF-MPI) were performed at 35 km grid spacing for the contiguous Mexico–U.S. domain (grid centroids are indicated as black crosses in Fig. 1) and boundary forcing was updated in 6-h intervals (Castro et al., 2012). The duration of the simulations covered the same period as the GCM forcing data. That is for MPI-ECHAM5, 1950–2100 and for HADCM3, 1968–2079. A

comprehensive evaluation of the WRF-MPI performance in the study region is presented in Shamir et al. (2014).

3.2. North American Regional Climate Change Assessment Program (NARCCAP)

NARCCAP (www.narccap.ucar.edu) is a multi-institutional community effort to produce high resolution climate projection simulations to explore uncertainties in regional scale projections of future climate and to generate climate change scenarios for use in impact assessment studies in North America (Mearns et al., 2007). Since they become available, NARCCAP data have been applied in a plethora of climate impacts studies, documented in more than 100 publications. Thus far NARCCAP consists of two phases. In phase I, dynamically downscaled simulations from meteorological reanalysis boundary conditions were conducted; and in phase II, similar simulations, but for IPCC A2 emission scenario, were performed to derive climate projections. Herein we used NARCCAP simulations from phase II.

NARCCAP used six different regional climate models (RCM) to downscale four Atmosphere–Ocean General Circulation Models for the historic period (1971–2000) and for projected future period (2041–2070), covering the conterminous United States and most of Canada. The NARCCAP RCM grid spacing is 50 km with 3-h reporting intervals. The four selected AOGCMs are the Canadian Global Climate Model version 3 (CGCM3), the NCAR Community Climate Model version 3 (CCSM3), the Geophysical Fluid Dynamics Laboratory (GFDL) Climate Model version 2.1 (CM2.1), and the United Kingdom (UK) Hadley Centre Climate Model version 3 (HADCM3), which is the same GCM as the one downscaled by UA-ATMO.

Assessment of the NARCCAP models for their skill in reproducing summer precipitation for the North American Monsoon system concluded that the GFDL model lacked the skill of providing adequate boundary conditions for RCM to simulate realistic climatology of summer rain in the Southwest (Bukovsky et al., 2013). Consequently, we decided to omit the GFDL model from our analysis and rely on the other three GCMs, each downscaled by two RCMs (total of six model simulations): WRFG-CCSM3, RCM3-CGCM3, HRM3-HADCM3, WRFG-CGCM3, RCM-CCSM and CRCM-CGCM3. The CCSM and CGCM3 were both reported to have dry summer biases and the HADCM3 was found to provide the most realistic boundary conditions as RCM forcing with early monsoon onset (Bukovsky et al., 2013).

It is noted that all selected four GCMs used in this study (MPI-ECHAM5, HADCM3 CCSM and CGCM3) have participated in all IPCC assessment reports and have established track records for simulating current and future climates. The equilibrium climate sensitivities of the four GCMs are within the full range of climate sensitivity for the models that participated in IPCC 2007 (Randel et al., 2007). Equilibrium climate sensitivity is a measure of the global climate system annual mean temperature change in response to a doubling of CO_2 after it has attained equilibrium. It is a commonly used index to represent the range of climate change projections obtained with different GCMs.

3.3. Climate projection results

The gauge observed total seasonal rainfall can be grouped into three wetness categories for both winter and summer (i.e. dry, medium and wet). The historical frequencies of the wetness categories were determined based on visual analysis of inflection points on the cumulative distribution curves of the seasonal total rainfall. The frequencies of the historic wetness categories are seen in Fig. 4 (left-most bars) for the winter and summer (left and right panels, respectively), and are used as reference to determine projected changes in the wetness category frequency.

The eight downscaled RCM simulations were compared for their frequency of winter and summer wetness categories for the periods available from NARCCAP (1971–2000 and 2041–2070). The rainfall values of the corresponding frequency bounds for each wetness category were identified in the RCM output for the *historical* (1971–2000) period for each RCM. Subsequently, the frequencies of these threshold rainfall values were then determined in the RCMs output for the *future* period (2041–2080) to identify the projected frequency of occurrence of the three wetness categories for the winter and summer.

Fig. 4 compares the results (left for winter and right for summer) for the eight different RCMs (from the second to the ninth bar) and for the historical period (left bar). The right-most bar shows the average frequencies of ensemble of the eight RCM models. For the summer season, seven models projected higher frequency of dry summers and six models projected lower frequency of wet summers. An outlier model that showed lower and higher frequency of dry and wet summers, respectively is the UA-ATMO WRF-HAD.

All eight models projected higher frequency of dryer winter and six of the models also projected higher frequency of wet winter. The average frequencies of the eight-model ensemble show that, on average, higher frequencies of dry summer and winter were projected, along with lower and higher frequencies of wet summer and winter, respectively.

The significance of the projected frequency of the seasonal wetness categories was tested and is summarized in Table 1. For this test, the empirical frequency distributions of the seasonal wetness

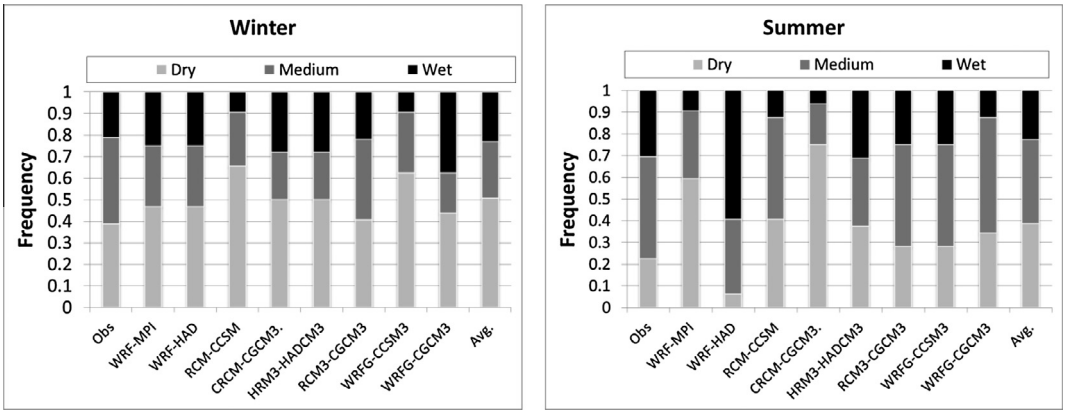

Fig. 4. The projected (2041–2080) frequency of wet, medium, and dry winter and summer (left and right panels, respectively). The frequency of the historical record and the average of the eight RCMs are also indicated in the left and right bars, respectively.

Table 1
Frequency of summer and winter wetness categories in the observed historical record, in the projections of the eight regional climate models, and in the average of the eight-model ensemble. The significance chance column indicates the percent of the climate model wetness categories that have greater dry and wet frequencies than the specific case of RCM model in the combined historical and future record.

	Significance (%)	Summer			Significance (%)	Winter		
		Dry	Medium	Wet		Dry	Medium	Wet
Observed record		0.266	0.468	0.306		0.387	0.403	0.210
WRF-MPI	0.6	0.594	0.312	0.094	7.2	0.469	0.281	0.250
WRF-HAD	4.2	0.063	0.344	0.594	13	0.469	0.281	0.250
RCM-CCSM	10.4	0.406	0.469	0.125	5.9	0.656	0.250	0.094
CRCM-CGCM3	1.9	0.750	0.188	0.063	13.1	0.500	0.219	0.281
HRM3-HADCM3	15.9	0.375	0.313	0.313	9.9	0.500	0.219	0.281
CRCM-CGCM3	46.2	0.281	0.469	0.250	45.1	0.406	0.375	0.219
WRFG-CCSM3	13	0.282	0.468	0.250	3.1	0.625	0.281	0.094
WRFG-CGCM3	4.9	0.344	0.531	0.125	1.1	0.438	0.188	0.375
Avg. multi-model		0.387	0.387	0.227		0.508	0.262	0.231

categories from the projections of the eight climate models were derived for the combined historic and future simulation periods. These distributions were derived by categorizing the seasonal wetness of 1000 randomly sampled (from a uniform distribution and with replacement) series, each 30 years, out of the combined historic and future periods (total 60 years). The significance values in Table 1 indicate the percent of the randomly sampled series with higher dry and wet frequencies than the specific RCM projection.

For example, for the summer WRF-MPI wetness categories, there is a very low chance (0.6%) that the distribution of the combined historic and future periods yield the same wetness category differences as the differences between the historic and future simulations. In the case of the summer WRF-MPI, the future change indicates more dry summers and fewer wet summers. Apart from the RCM3-EGCM3, which has a high percentile significance (greater than 45%) that the future projection is indistinguishable from the combined record, for all other model projections there is less than 16% chance (and in some cases much less) that the wetness categories of the future projections could have been derived from the combined simulation record.

The performance difference between the downscaled simulations of the UA-ATMO WRF-HAD and the NARCCAP HRM3-HADCM3 is attributed to the spectral nudging, which is a method that conserves synoptic scale variability from GCMs to RCMs and affecting the RCMs representation of convective precipitation (Castro et al., 2012). The UA-ATMO WRF-HAD implemented a spectral nudging methodology while NARCCAP HRM3-HADCM3 did not. Although the HADCM3 model has relatively wet biases, which were conserved by the spectral nudge approach, it was reported to capture well the climatic features over the North American Monsoon region (Geil et al., 2013).

Geil et al. (2013) assessed the skill of the recently released CMIP5 (IPCC Assessment Report 5) models to represent the climatological features of the North American Monsoon region. They concluded that for most GCMs there was no marked performance improvement compared with the GCMs available from the CMIP3. However, they identify additional GCMs that simulated realistic climatology of precipitation for the region. Cook and Seager (2013) found that the ensemble mean of all CMIP5 models represents well the onset period of North American monsoon precipitation. However, most CMIP5 models are too wet during the retreat period of the monsoon season. These performance results are consistent with the conclusion of the NARCCAP analysis (Bukovsky et al., 2013).

Additional analysis was performed to detect other precipitation features with clear differences between the historical and future WRF-MPI simulation spans. The only considerable difference detected between the historic and future periods is for the duration between rainfall events (inter-arrival time) in summers that are categorized as dry. This suggests that the projected future dry summers are dryer than the historic dry summers. This increase in the time between storms in dry summers is attributed mainly to a projected delay of the monsoon onset. No clear differences were found for other precipitation features, such as the magnitude of precipitation, distribution of storm duration and total number of storms events.

3.4. Comparison with GCM and statistically downscaled realizations

In this study we generated climate projection scenarios for hydrologic impact assessment that are informed by selected simulations of well performing dynamical downscaled models. We recognize that there are competing approaches and detailed discussion regarding the merit of the various approaches for the region of interest is beyond the scope of this manuscript. However, in this section we assess whether using other commonly available climate projections would have yielded similar conclusions as was reached by the eight dynamically downscaled models with respect to the projected changes in the seasonal wetness categories.

As mentioned in Section 1.1, Reclamation provides time series of precipitation from CMIP3 and CMIP5 for the contiguous U.S. (Reclamation, 2011; url: gdo-dcp.ucllnl.org). This dataset includes GCM output resampled to a gridded 1° and 2° resolution for the CMIP5 and CMIP3, respectively. The GCM output includes historic and projection periods for 134 CMIP5 and 112 CMIP3 GCM. The CMIP3 [CMIP5] simulations consists of ensembles from 15 [18] GCMs for A1b, A2 and B1 [RCP2.6, RCP4.5, RCP 6.0 and RCP8.5] future emission scenarios. These GCM simulations were further bias adjusted and statistically downscaled to produce 1/8° resolution of daily precipitation simulations. The daily precipitation bias adjustment procedure is based on the bias corrected–constructed analogs method (BCCA; Maurer et al., 2007) and detailed description of the downscaling method is in Brekke et al. (2013).

In Figs. 5 (for summer) and 6 (for winter), we show rainfall projection information for 134 CMIP5 and 112 CMIP3 (left and right, respectively) of the coarse GCMs (upper panels) and the 1/8° statistically downscaled simulations (lower panels). The frequencies for both the wet and dry summers/winters are shown with the medium seasonal frequency inferred as the difference between 1 and the sum of the dry and wet frequencies. The solid black lines that form four quadrants indicate the wet and dry frequencies of the historical observed record, as also indicated in Fig. 4 (left bars) and Table 1. The shaded gray quadrants indicate the consensual projected change, as interpreted from the eight dynamically downscaled models. That is, projected increase [decrease] in frequency of dry [wet] summers (lower right quadrant, Fig. 5); and increase in frequency of both dry and wet winters (upper right quadrant, Fig. 6). The gray dots indicate the results of each of the 134 CMIP5

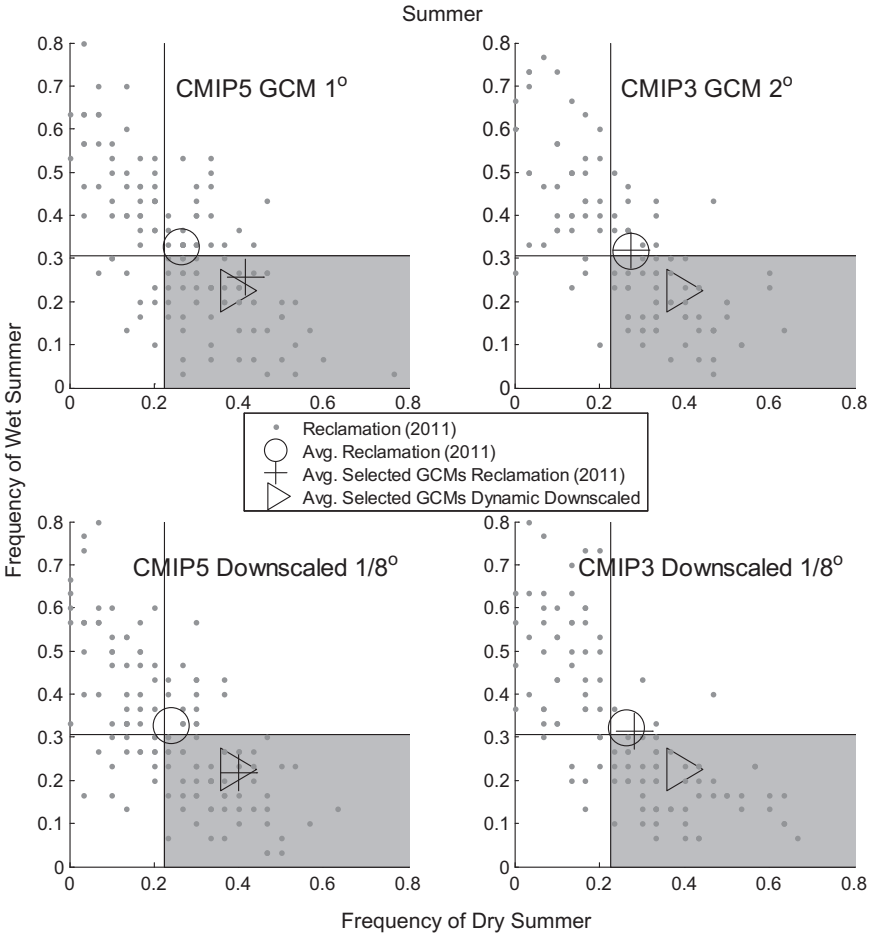

Fig. 5. Frequency of projected dry versus wet summer for the Upper Santa Cruz region (2041–2070). The black lines indicate the frequency of the observed historical records and the gray shade indicate the quadrant in which most (or all) of the eight dynamically downscaled models projected change in the frequency of their wetness categories of dry and wet seasons. The upper panels are resampled 1° of 134 CMIP5 models projections (left) and 2° of 112 CMIP3 models projections (right). The lower panels are 1/8° statistically downscaled of the CMIP5 (left) and CMIP3 (right) (gray dots). The open circles indicate the multi model averages of all GCMs, the triangles are for the dynamic downscaled models and the pluses are the multi model average of the four selected GCM with the comparable emission scenario (A2 and RCP85 for the CMIP3 and CMIP5, respectively).

and 112 CMIP3 model projections (2041–2070) from Reclamation (2011) and large open circles indicate their multi-model average. The triangle markers represent the multi model average of the selected dynamically downscaled models and the average multi model of the same selected GCMs simulations with either A2 (for CMIP3) or RCP85 (for CMIP5) green-house gas emission scenarios, available from Reclamation are indicated by the plus markers.

A first notable result is that very similar conclusions with respect to changes in the dry and wet frequency can be drawn for both summer and winter from the coarse GCMs (upper panel) and the bias adjusted statistically downscaled projections (lower panels). However, the CMIP3 and CMIP5 simulations display considerable differences in their multi-model projected wetness categories.

For the summer, the CMIP3 and CMIP5 multi-models are very similar to the observed record, with a slight increase in the frequency of dry summers (open circles). In addition, the mean of the selected statistically downscaled simulation of the CMIP5 yields a similar conclusion for the direction of the projected change as concluded by the dynamically downscaled projections (plusses and triangles, respectively). For the CMIP3 models, the CCSM model simulation projected a decrease [increase] in dry [wet] summer frequencies, which caused the multi-model average result of the selected GCMs (plusses) to be outside of the quadrant of the projected change by the dynamically downscaled simulations.

The multi model average of the GCMs might not represent well the projections of all the GCMs for the summer. It is seen in Fig. 5 that the results for most of the GCMs are either increase [decrease] frequency of wet [dry] (upper left quadrant), or decrease [increase] frequency of wet [dry] summers (lower right quadrant). The average multi models aggregates these two distinctively different GCMs' results to yield a projection of increase of dry and wet frequency (upper right quadrant), which is different from most of the GCMs projections.

For the winter, the CMIP5 GCM 1° showed the multi-model average for the selected GCMs in the same quadrant of change as the dynamically downscaled model; and the CMIP5 1/8° statistically downscaled multi-model average showed a slight decrease in the frequency of dry winters. The multi-model average of the selected GCMs shows an increase in dry winters and decrease in wet winters for both CMIP3 and CMIP5. For the GCM3 both selected models and the multi-models showed an increase [decrease] of the dry [wet] category. In contrast to the results from the summer, the average multi model for the winter represents well the conclusion from most of the GCMs (lower right quadrant).

Table 2 reports the percent of future simulations (2041–2070) by Reclamation's models with frequencies of wet and dry season that have changes move in the same direction of change seen for the projections of the selected dynamically downscaled models.

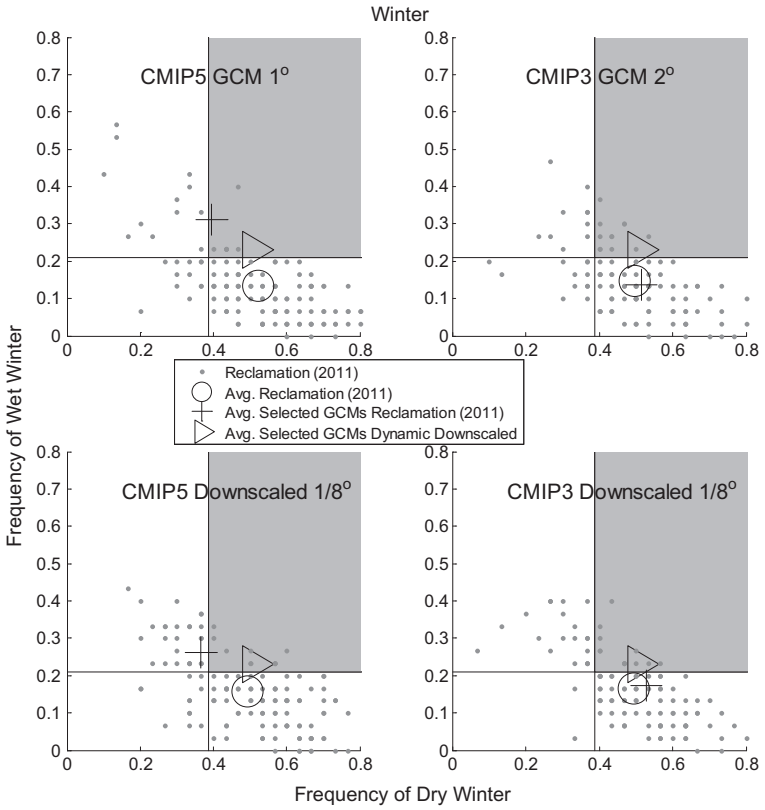

Fig. 6. As described in Fig. 5 but for the winter.

Table 2
Wetness category summary of 134 realizations of CMIP-5 sampled at 1° and statistically downscaled to 1/8° and 112 realizations of CMIP-3 sampled at 2° and statistically downscaled to 1/8° for the Nogales Gauge location. The values indicate percent of realizations that the future simulation (2041–2070) has wetness frequency as concluded from the eight dynamically downscaled models (i.e. higher and lower frequency of dry and wet summer; higher frequency of dry and wet winter). The columns represent each wetness category independently and the dependent frequency (both conditions for dry and wet categories are projected). CMIP data was retrieved from gdo-dcp.ucllnl.org.

Summer	Higher freq. of dry (%)	Lower freq. of wet (%)	Higher freq. of dry and lower freq. of wet (%)
CMIP5 resampled unadj. GCM 1°	60	49	42
CMIP3 resampled unadj. GCM 2°	63	57	52
CMIP5 bias adj. downscaled 1/8°	54	54	43
CMIP3 bias adj. downscaled 1/8°	54	58	51
Winter	Higher freq. of dry (%)	Higher freq. of wet (%)	Higher freq. of dry and wet (%)
CMIP5 resampled unadj. GCM 1°	82	13	7
CMIP3 resampled unadj. GCM 2°	80	20	11
CMIP5 bias adj. downscaled 1/8°	72	29	7
CMIP3 bias adj. downscaled 1/8°	80	29	11

Differences are seen for changes in either dry or wet categories, or both dry and wet categories. For instance, the dynamically downscaled models projected a higher frequency of dry summers and lower frequency of wet summers. It is seen that 60% [49%] of the 134 unadjusted and resampled to 1° CMIP5 GCMs projected a higher frequency of dry summers [lower frequency of wet summer]. However, only 42% of the realizations show both a higher frequency of dry summers and lower frequency of wet summers. For the winter the dynamically downscaled models indicated an increase in the frequency of both dry and wet winters. The GCMs clearly project an increase in the frequency of dry winters (82%); however, only 13% of the realizations indicate an increase in the frequency of wet winters and only 7% of the realizations indicate an increase of both dry and wet winters.

Again it seen that the differences between CMIP5 and CMIP3 for the GCMs and the bias corrected downscaled series are smaller than 10%. In addition, the differences between the GCM and the bias corrected statistically downscaled simulations are fairly small (less than 16%).

The analysis presented in this section clearly shows that the results obtained by the eight dynamically downscaled projections from the four selected GCMs for inference on wetness category are in several cases in line with the broader set of GCM results examined in this section but there are also substantial differences.

4. Hydrologic modeling framework

The utility of the hydrologic modeling framework was previously demonstrated to assess the impact of increasing groundwater withdrawal due to projected population growth on the base flow in the Santa Cruz River near Tumacacori, which is downstream of the study area (about 35 km northwest from the Nogales

Gauge) (Nelson, 2010). In addition, the hydrologic modeling part of the framework was used in assessing the impact of long term climate variability as interpreted from a ~300 year rainfall reconstruction developed for the study area from tree-ring records (Shamir et al., 2007b).

The hydrologic modeling framework used in this study consists of the hourly precipitation weather generator, rainfall runoff transformation model that produces synthetic hourly streamflow at the international border crossing, a streamflow channel routing network that simulates channel transmission losses and groundwater recharge, and a simplified groundwater model for the four microbasins (Fig. 7). The models used in this study enhance those reported in Shamir et al. (2005, 2007a) with parameters updated using an additional 10 years of precipitation and streamflow observation data. For the interested reader, a detailed description of the hydrologic model modifications and the revised parameters are in Shamir (2014). In the following we outline the modeling components.

4.1. Hourly rainfall generator

The rainfall generator produces hourly rainfall using stochastic point process theory (e.g., Snyder and Miller, 1997). An ensemble of synthetic likely rainfall scenarios represents the regional rainfall characteristics, natural variability and associated uncertainties. The rainfall generator was set to simulate four seasons: fall (October), winter (November–March), spring (April–June) and summer (July–September). As mentioned in Section 3, the summer and winter rainfall generator components were further divided into three wetness categories (i.e., wet, medium and dry). Dry summers [winters] are identified in the historical data as seasons that were dryer than 160 [70] mm and wet summers [winters] are seasons that were wetter than 260 [140] mm. For each wetness category, the rainfall generator produces likely hourly scenarios by sampling from statistical distributions that represent: (a) the time duration between storms; (b) the duration of the storm events, including the distribution and number of hourly rainfall pulses during the storm event, and (c) the magnitude of the hourly precipitation.

Although large precipitation events have occurred in October, in most years the fall and spring were relatively dry with infrequent small precipitation events. For these seasons we used exponential distributions to characterize the occurrence of hourly precipitation magnitude.

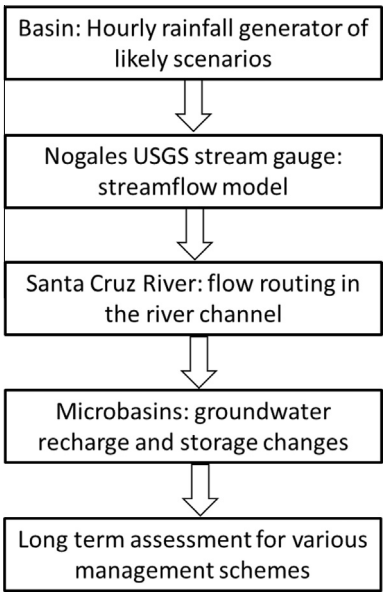

Fig. 7. Schematic of the sequencing and links of the components of the hydrologic modeling framework.

4.2. Modifying the rainfall generator to reflect climate projections

We used the eight selected dynamically downscaled climate models to identify the projected frequency of the wetness categories for both winter and summer. A potential caveat of this procedure is the underlying assumption that the future characteristics of rainfall within wetness categories will be similar to the characteristics of those in the observed historical record. In other words, in this approach the projected change in the future is the frequency of occurrence of the various wetness categories and the rainfall regime within a category will have similar characteristics to those observed in the historic record.

As mentioned in Section 3.3, the analysis of the eight selected regional climate models did not reveal considerable differences between the historic and future simulations of the rainfall characteristics within a wetness category. In order to estimate the wetness frequency for winter and summer in the RCM future simulations (2041–2070), we first identified the total winter and summer threshold values that define the transition between wetness categories in the simulations of the historical period (1971–2000) and yield similar frequencies to the wetness categories in the observed record. These transition threshold values found in the historical simulations are then examined in the future simulations to assign the projected future frequencies of the wetness categories. An additional case is a multi-model ensemble that is based on the arithmetic average of the eight projected frequencies of the dynamically down scaled simulations. The projected frequencies that were used in the rainfall generator to represent the projected future change in the wetness categories seasonal frequency are presented in Fig. 4 and comparison among these frequencies is discussed in Section 3.3.

4.3. Conceptual hydrologic model

A conceptual hydrologic model was developed in order to transform the sequences of hourly rainfall realizations to hourly streamflow that represents the variability and characteristics of the historic streamflow record at the Nogales stream gauge. The model structure was constructed to represent the different hydrologic responses between winter and summer.

The Arizona Department of Water Resources (ADWR) developed a detailed Modular Finite Differences Groundwater Flow Model (MODFLOW) that simulates changes in groundwater levels for the southern four microbasins (Erwin, 2007). The execution of the spatially distributed MODFLOW requires distributed groundwater data and boundary conditions (e.g. streamflow, recharge and evapotranspiration data) and significant CPU time for execution. In this study, we used a simplified version of groundwater model as in Shamir et al. (2005, 2007a) modified herein for hourly runs (Shamir, 2014).

The groundwater model is set to represent the microbasins as a series of four spatially lumped and disconnected reservoirs. The parameters for this model were estimated from the aquifer characteristics reported in Erwin (2007). Using the ADWR MODFLOW model simulations, the depth-to-water in the microbasins is estimated as a linear function of the relative in-storage water in the microbasins. Thus, the simplified groundwater model provides an effective depth-to-water estimate for the microbasins that does not represent the spatial variability of the ground water level.

The routing of the hourly streamflow along the river channel to the next downstream microbasin is estimated as the remaining hourly flow after groundwater recharge is deduced. The rate of

groundwater recharge of a given microbasin is dependent on the infiltration rate coefficient and the groundwater in-storage in the microbasin. In addition, the area where recharge occurs was considered as a function of the wetted width of the channel.

The wetted width of the channel was estimated from the cross section survey data of the channel wetted width during different flow rates at the Nogales stream. The potential recharge volume for each microbasin was then estimated as a function of the infiltration rate, wetted channel width, and the length of the channel in the microbasin.

5. A water resources management case study

5.1. Stakeholder engagement process

The link between the use of the modeling framework described above and groundwater management was made through engagement of stakeholders in the development of management questions for analysis. The stakeholders represented a cross-section of the community, including water utility managers, federal and state agency personnel, consultants, attorneys, academic researchers, and representative from non-governmental organizations and local entities. In a series of three workshops, the project team iteratively introduced climate and modeling concepts, as well as management policies and practices, and elicited feedback on questions to pose during the modeling exercise. Information about the workshops and the stakeholder engagement process is in (https://wrrc.arizona.edu/GCASE).

5.2. Case study development

The effectiveness of the hydrologic modeling framework for water resources planning and management was demonstrated through a case study that assumes various water management scenarios. The municipal potable water supply for the city of Nogales, Arizona is the main withdrawal from the microbasins. In order to satisfy its entire need, the City of Nogales alternates between the microbasins and the Portrero well-field which is a deeper aquifer with steadily declining water levels and lower water quality that also requires arsenic removal (Alejandro Barcenas, City of Nogales, personal communication). The City's total annual average consumption for 1990–2009 was about 4200 ac-ft yr^{-1} (5.2 Mm^3 yr^{-1}), ranging from 3800 to 4800 ac-ft yr^{-1} (4.7–5.9 Mm^3 yr^{-1}) (ADWR, 2012). This annual consumption was split approximately evenly between the Portrero well-field and the microbasins. The 2025 water demand for the city of Nogales is projected to remain below 5000 ac-ft yr^{-1} (6.2 Mm^3 yr^{-1}) (ADWR, 2012).

We evaluated three proposed annual groundwater withdrawal goals from the microbasins of 2000, 3000 and 5000 ac-ft yr^{-1} (~2.47, 3.7, and 6.17 Mm^3 yr^{-1}, respectively). The monthly withdrawal rate from each of the microbasins is assigned proportionally to the monthly distribution withdrawal reported in Erwin (2007).

The Santa Cruz Active Management Area mission statement is to "manage all water resources in the AMA conjunctively, to assure a reliable water supply for current and future uses, and to protect aquatic and riparian habitat while sustaining a healthy economy" (http://www.azwater.gov/azdwr/watermanagement/amas/santacruzama).

To address this challenge, maximum depth-to-water thresholds have been proposed to assist in defining the management goals (e.g. Corkhill and Dubas, 2007). An alternative approach is to maintain various low flow characteristics (e.g. frequency, duration) in gaining channel reaches (Nelson, 2010).

In Arizona commonly studied riparian species include the *Populous fremonti*, *Salix gooddingii*, *Tamarix ramosissima*, and the *Prosopis velutina*. A spectrum of studies provides robust quantifications of the flow needs and flow responses of the different species. The two most studied basins in Arizona are the Santa Cruz River basin and the San Pedro River basin, immediately to the east of the Santa Cruz watershed (Nadeau and Megdal, 2012).

Sustaining riparian health requires avoidance of severe groundwater decline. Several studies were conducted to identify riparian vegetation characteristics and resiliency to variety of stressors (e.g. Stromberg et al., 2012; Shafroth et al., 1998; Lite and Stromberg, 2005; Snyder and Williams, 2000). Identifying water level impact on riparian ecosystems is dependent on the vegetation species, the age of the plants, and hydrologic and meteorological conditions. Plant mortality might be dependent of the depth of water level decline, the timing of decline, the frequency of stress, duration below a threshold, and the rate of change. Stromberg et al. (2009) for example, reported that the maximum groundwater depth to sustain adult *P. fremonti* communities underlining the San Pedro riparian corridor is 4–6 m. At present however, there are no well-defined set of guidelines that can be used for water resources management as a general guide for groundwater levels that sustain riparian health.

For this study we evaluated three groundwater level thresholds as critical depths below which groundwater withdrawal from a microbasin were terminated in order to maintain riparian health. The thresholds were set to 10, 20 and 30 ft depth to water (~3, 6 and 9 m, respectively). Our selection was designed to represent three riparian vegetation mortality levels of risk that a water management plan might consider. As mentioned above, the groundwater threshold values are effective depth-to-water that represents aggregated water levels for the entire microbasin surface area. These thresholds do not consider the spatial variability of the groundwater level in the aquifer.

To summarize the case study design, we developed nine management scenarios that include three annual pumpage goals and three groundwater thresholds. In each of the microbasins the withdrawal ceased when the groundwater level fell below the assigned groundwater threshold. The hydrologic modeling framework was executed to generate 10 ensembles of synthetic rainfall for each of the nine management scenarios; each ensemble had 100 realizations and each realization consisted of 62-years of hourly rainfall. The 10 ensembles include a reference ensemble that is based on the historical record, eight ensembles that represent the projected change from the eight regional climate models, and another ensemble that represents the average change of the eight climate models.

6. Case study results and discussion

The hydrologic modeling framework simulated ten ensembles for each of the nine management scenarios producing a large amount of model output and time series that include information on the aquifer water table, groundwater recharge, streamflow, and precipitation. This simulated dataset can potentially be queried to answer many questions concerning the reliability of the various management scenarios to achieve their stated goals, recurrence intervals of specific events, the impact of natural variability, and assessment of the projected impact from climate change. The results discussed in the following are selected pertinent and interesting examples as identified in the stakeholders workshops.

In Fig. 8, we evaluate the water supply reliability to pump a specified annual volume of water at various assumed annual withdrawal rates (2.47, 3.7 and 6.17 Mm^3 yr^{-1} for the left, center, and right panels, respectively) and depth-to-water thresholds (3, 6 and 9 m). In Fig. 8, and also Figs. 9–12, the length of the vertical lines represents the 5–95 percentiles range and the asterisks repre-

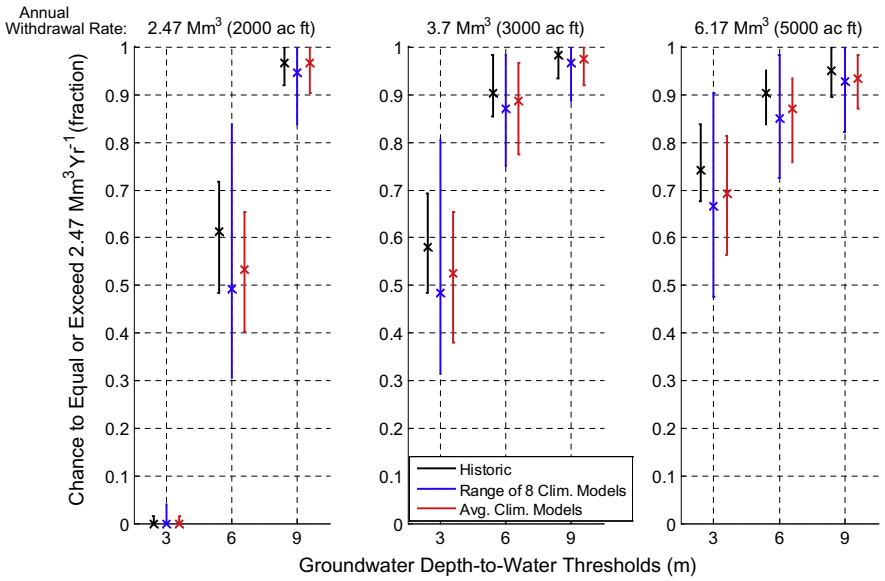

Fig. 8. The reliability to attain or exceed an annual withdrawal goal of 2.47 Mm^3 (2000 ac-ft) from the microbasins (based on assumed annual groundwater withdrawal rates and depth-to-water thresholds). The lines indicate the 5 and 95 percentile range of the ensembles (medians are indicated as asterisks). The baseline ensemble that represents the historic record, eight ensembles that reflect climate projections and average climate projection are indicated in black, blue, and red, respectively. (For interpretation of the references to color in this figure legend, the reader is referred to the web version of this article.)

sent the median of the ensembles. The black lines denote the reference ensemble that represents the historical record, the blue lines represent the combined eight climate projection ensembles, and the red lines are for the ensemble of the average of the climate model projections.

The reliability of pumping 2000 ac-ft yr^{-1} (2.47 Mm^3 yr^{-1}) for the nine different management scenarios varies significantly as a function of the selected annual withdrawal rate (2000, 3000 or 5000 ac-ft yr^{-1}) and is severely affected by projected climate change (Fig. 8). As expected, larger annual withdrawal rates are generally more effective in capturing larger volumes of stream recharge, and deeper depth-to-water thresholds increase the reliability to attain or exceed every-year the annual goal of 2000 ac-ft yr^{-1}. However, even with these reliability-favorable management scenarios, the reliability is in the range 90–100%, with medians that are lower than 100%. The future climate projections, as indicated both by the eight ensembles (blue) and the average of the climate projections (red) increase the uncertainty (spread) in the reliability to meet the annual goal withdrawal. The reliability of the lower bounds and the medians (asterisks) are considerably lower than the reference ensemble. We note that although the eight climate model show increase in the upper bounds, the combined ensemble members yield a positively skewed distribution that was caused by the outlier results of the UA WRF-HAD rainfall simulation, as discussed in Section 3.

The capability of the hydrologic framework to analyze the prospective water shortage from the microbasins is demonstrated in the next set of results. In Fig. 9, we assess the likely total deficit

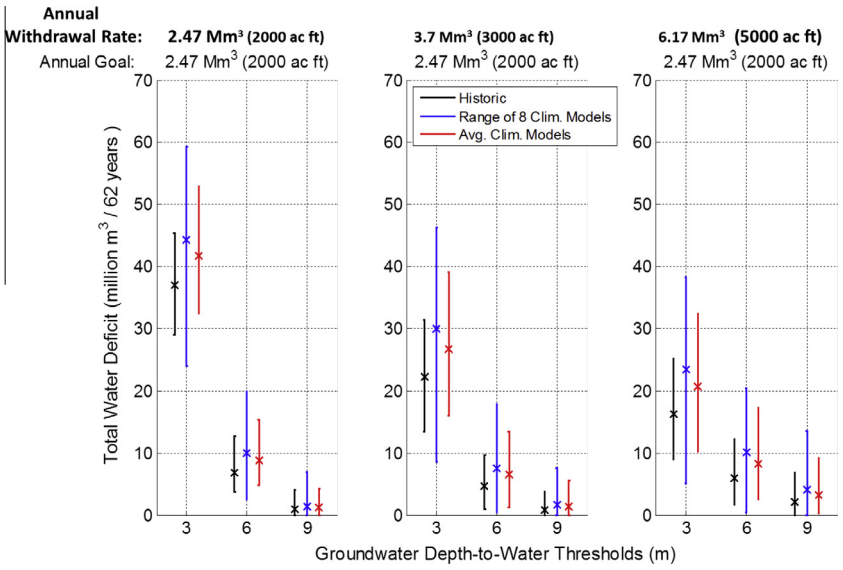

Fig. 9. The total 62-year cumulative deficit below the annual goal of 2.47 Mm^3 (2000 ac-ft) using three different annual withdrawal rates. Lines represent the 5–95 percentile ranges as explained in Fig. 8.

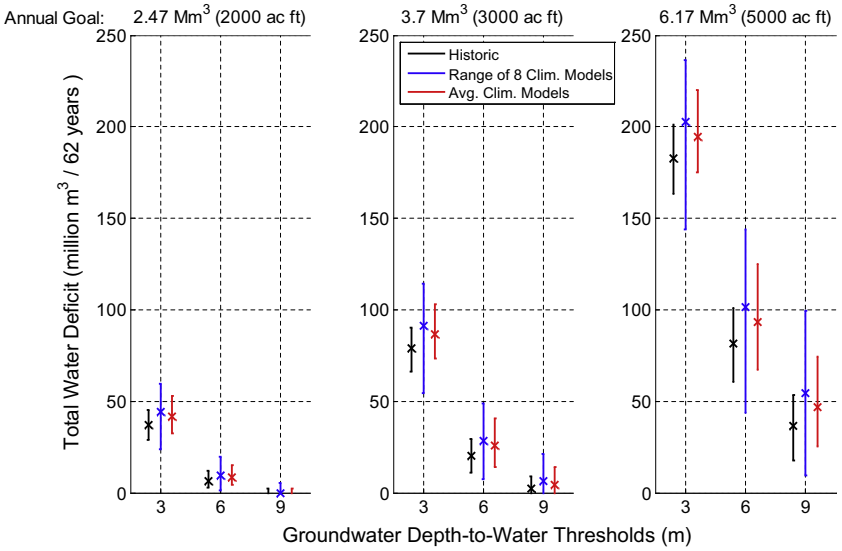

Fig. 10. The total 62-year cumulative deficit below the annual withdrawal goal (2.47, 3.7 and 6.17 Mm^3 [2000, 3000 or 5000 ac-ft]). Lines represent the 5–95 percentile ranges as explained in Fig. 8.

over the 62-year simulation period by summing the deficit in years that the annual pumping goal of 2000 ac-ft yr^{-1} was not attained. Similarly, Fig. 10 presents results of the cumulative deficit, but in this case, for the cumulative deficit years that the specific annual withdrawal goal was not attained. Again the annual groundwater withdrawal goal, the simulated groundwater withdrawal rates and the groundwater thresholds controlled the total deficit and their spread. It is seen that assigning the 9 m threshold yields a relatively small deficit and the deficit increases as the threshold is assigned to a shallower value. The climate change projections have a larger spread of long-term deficit and the medians are higher compared with the historic ensemble.

Inspecting the cumulative deficit, compared to the annual withdrawal goal (Fig. 10), shows the general increase in deficit with increasing annual withdrawal goal. In addition, the climate projections for all management scenarios are expected to increase the cumulative water deficit and increase uncertainty.

To provide perspective for these deficit values, we note that the average winter and summer flow at the Nogales gauge (Fig. 3) were 9.1 and 9.6 $Mm^3\ yr^{-1}$ (7400 and 7800 ac-ft yr^{-1}, respectively).

It is prudent to compare these long term deficit assessments with the projected availability of streamflow and the streamflow recharge to the microbasins. The range of total recharge that occurred over 62 years is plotted in Fig. 11. It is apparent that the groundwater recharge is also a function of the water management scenario. In general, the projected recharge increases when the management scenario allows for higher withdrawal either because of annual withdrawal rates, or deeper depth-to-water thresholds. In other words, drawing down storage in the microbasins enhances the groundwater recharge from streamflow (that is,

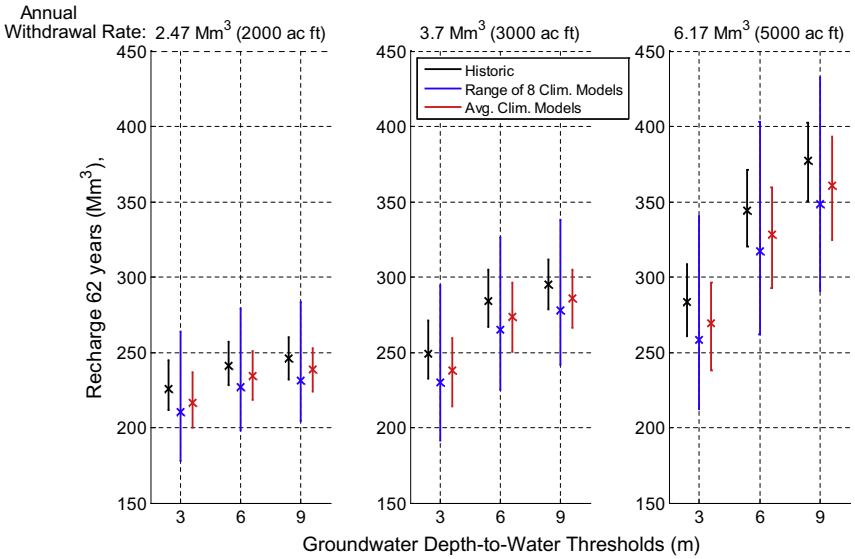

Fig. 11. The total 62-year cumulative groundwater recharge from streamflow transmission loses to the microbasins ($10^6\ m^3$). Lines represent the 5–95 percentile ranges as explained in Fig. 8.

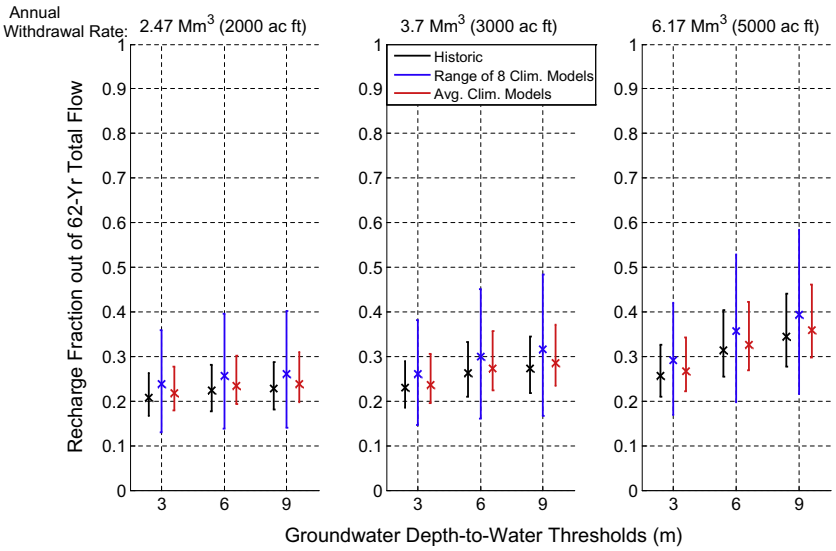

Fig. 12. The ratio between cumulative 62 years of groundwater recharge and streamflow. Lines represent the 5–95 percentile ranges as explained in Fig. 8.

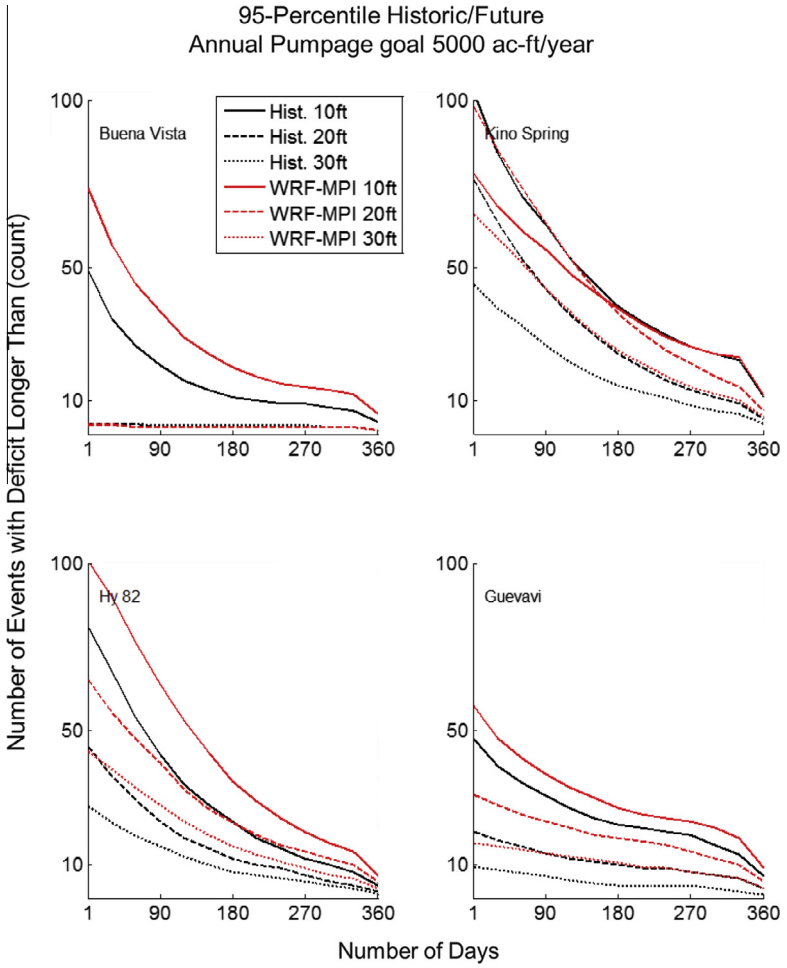

Fig. 13. The occurrence count during 62 years that the groundwater levels in each of the four microbasins (four panels) were below the threshold for a consecutive number of days for the case of 5000 ac-ft annual withdrawal goal. In each panel, the 95th percentile of the ensemble is shown for the baseline ensemble (black) and the projected WRF-MPI ensemble (red). The different groundwater level thresholds are shown as different lines shapes. (For interpretation of the references to color in this figure legend, the reader is referred to the web version of this article.)

induces recharge). This implies that the management scenario affects the amount of water that is retained and recharged into the microbasins. The projected climate change is expected to decrease the central mode of recharge, increase the range of variability and significantly reduce the lower bound.

Next, we examine the fraction of the actual calculated groundwater recharge as a fraction of the streamflow (Fig. 12). Using the historic ensemble to project future streamflow, the recharge is estimated to range from as low as 17% when a 2000 ac-ft yr^{-1} annual withdrawal goal and annual withdrawal rate are assumed to upward of 44% when a deep depth-to-water threshold and 5000 ac-ft yr^{-1} annual withdrawal rates are assessed. The inclusion of the climate projection analyses increases the recharge range to 13–58%. The analysis of recharge from streamflow in ephemeral rivers has to be considered while inspecting the temporal characteristics of the flow events. The optimal events for recharge are medium in magnitude (yet they fully wet the maximum channel area) and comparatively long in duration. Large, sporadic flow events often tend to be of shorter duration and lack the residence time for maximum recharge.

Last, in response to specific questions from water management stakeholders, we present an analysis that shows the frequency and duration for a given microbasin to be below the assigned threshold. We note that the different physical characteristics of the microbasins (Erwin, 2007) cause differences in their hydrologic response as demonstrated in Shamir et al. (2007b). This analysis could also be used to provide information concerning the expected statistical distribution of the recovery for given microbasin for a given management scenario. The example in Fig. 13 is shown for the three thresholds and the annual withdrawal goal of 5000 ac-ft yr^{-1} (6.17 Mm^3 yr^{-1}). In Fig. 13 the 95th percentiles of the base line ensemble (black) and the UA WRF-MPI ensemble (red) are shown for the four microbasins. We used the 95th percentile as the conservative measure that is thought to be relevant for a water resources management.

It can be seen from the example that for the Buena Vista basin, there were about 50 and 75 cases where the water level declined below 3 m (10 ft) and the decline lasted less than two days for the historic and WRF-MPI scenarios, respectively. Moreover, there were about 10 and 15 cases when the decline below 3 m lasted more than 270 consecutive days for the historic and WRF-MPI scenarios, respectively. Two notable conclusions drawn from this analysis are (1) the projected climate change increases the time when water level is below threshold, and (2) the microbasins react differently to a given operational scenario. For example, it can be seen that the Buena Vista rarely declines below the threshold 3 and 6 m (10 and 20 ft), while Kino Spring declines below the thresholds for all management scenarios.

In summary, through this case study analysis we demonstrated the importance of water management scenario development to achieve high reliability in the annual delivery, control the cumulative deficit, and optimize the recharge to the microbasins. These are, of course, competing objectives and a compromise threshold that balances these competing objectives will be needed to yield optimal and sustainable operation of the microbasins.

7. Conclusions and recommendations

The impact of projected future climate on the local water resources in the Upper Santa Cruz River was examined in this study. The analysis of precipitation projections for the study area from the eight selected well-performing dynamically downscaled GCMs concluded that the major difference between the simulation of the historic and future periods is the frequency of the summer and winter three seasonal wetness categories. The projected future summer regime is expected to have higher [lower] annual frequency of the dry [wet] seasons. The future climate projections for the winter point to increased frequency of both dry and wet winters and a decrease in frequency of medium winters.

These projected changes in wetness category frequencies were compared to climate model realizations readily available from Reclamation (2011). It was concluded that the selected models represent a subset of model scenarios that do not necessarily agree with the multi-model ensemble average. The multi-model ensembles of the Reclamation's projections indicate an increase in the frequency of dry summers and winters and no change [decrease] in the frequency of wet summers [winters]. However, the Reclamation's multi-model averages of the selected CMIP5 GCMs indicate similar summer trend of change to the dynamically downscaled.

We used a hydrologic modeling framework to assess the impact of the projected climate on the local microbasin water resources using a case study that examined nine management plans, different in their annual withdrawal rates and groundwater depth-to-water thresholds that prompt withdrawal termination. We concluded that water supply reliability, long term accrued water shortage, groundwater recharge rate during streamflow events, and the recovery frequency of water level to rise above the depth-to-water thresholds are all strongly dependent on the selected management plan.

In addition, the projected future climatic impact is expected to further complicate the water resources management tasks because of the increased uncertainty in the future of precipitation. The median results of the ensembles simulations that represent the climate change impact indicated decrease of water supply reliability, increase of the long term water shortage, decrease of the groundwater recharge from streamflow, and longer periods of groundwater level below the depth-to-water thresholds.

The considerable impact of the water resources management plan and the projected climate change on the state of the microbasins, points to the importance of careful selection of an operational management plan in order to achieve long-term sustainable conditions. It is prudent to identify a plan that optimizes a priori set of objectives that consider water supply reliability issues in conjunction with preservation of healthy riparian assets. The hydrologic modeling framework presented herein can be used to support water managers in the development of an optimal set of management plans that assess the tradeoffs among these objectives.

Various methods for assessing climate change impact on water resources have been reported in the scientific literature (e.g., Wilby and Wigley, 1997). It is advisable however to evaluate each method and identify its suitability for the objectives of the specific region and the pertinent questions at hand. We believe that the method used in this study can provide useful results for a region that meets the following criteria: the local climate is a major component of the region's water resource; the high temporal resolution and the characteristics of episodic events is a dominant factor of the region's hydrologic regime; hydrologic inputs such as rainfall and streamflow are highly variable and difficult to predict; future climate projections indicate increased variability and uncertainty; and datasets are available to understand the climate variability of the region at the scale of interest.

Our research team is currently engaged in studying the transferability of the presented procedure and assessing its applicability to assess impact of projected climate change on local water resources in other regions.

Acknowledgments

Funding for this work was provided by U.S. National Oceanic and Atmospheric Administration, Sectoral Application Research Program (Award number NA12OAR4310092). The research work

was also partially supported by the Hydrologic Research Center Technology Transfer Program. Special thanks are extended to Mike Lacey, Arizona Department of Water Resources, Alejandro Barcenas, City of Nogales, James Leenhouts and James Callegary, U.S. Geological Survey, Greg Kornrumph, Salt River Project, Perez Luna Guillermo, Conagua, Mexico and two anonymous reviewers who provided constructive input that improved this manuscript. The opinions expressed herein are those of the writers and do not reflect those of the funding agency or the individuals acknowledged.

References

ADWR, Arizona Department of Water Resources, 2012. Demand and Supply Assessment 1985–2025. Santa Cruz Active Management Area, July 2012.

Brekke, L., Thrasher, B.L., Maurer, E.P., Pruitt, T., 2013. Downscaled CMIP3 and CMIP5 Climate Projections: Release of Downscaled CMIP5 Climate Projections, Comparison with Preceding Information and Summary of User Needs. U.S. Department of Interior, Bureau of Reclamation, Tech. Rep., 116 pp.

Bukovsky, S.M., Gochis, D.J., Mearns, L.O., 2013. Towards assessing NARCCAP regional climate model credibility for the North American monsoon: current climate simulations. J. Clim.. http://dx.doi.org/10.1175/JCLI-D-12-00538.1.

Carleton, D., Carpenter, A., Weber, P.J., 1990. Mechanisms of interannual variability of the Southwest United States summer rainfall maximum. J. Clim. 3, 99–1015.

Castro, C.L., Pielke Sr., R.A., Adegoke, J.O., 2007a. Investigation of the summer climate of the contiguous U.S. and Mexico using the regional atmospheric modeling system (RAMS). Part I: model climatology (1950–2002). J. Clim. 20, 3866–3887.

Castro, C.L., Pielke Sr., R.A., Adegoke, J.O., Schubert, S.D., Pegion, P.J., 2007b. Investigation of the summer climate of the contiguous U.S. and Mexico using the regional atmospheric modeling system (RAMS). Part II: model climate variability. J. Clim. 20, 3888–3901.

Castro, C.L., Chang, H., Dominguez, F., Carrillo, C., Kyung-Schemm, J., Juang, H.H.-M., 2012. Can a regional climate model improve warm season forecasts in North America? J. Clim. 25, 8212–8237. http://dx.doi.org/10.1175/JCLI-D-11-00441.1.

Cook, B.I., Seager, R., 2013. The response of the North American monsoon to increased greenhouse gas forcing. J. Geophys. Res. 118, 1690–1699.

Corkhill, F., Dubas, L., 2007. Analysis of Historic Water Level Data Related to Proposed Assured Water Supply Physical Availability Criteria for the Santa Cruz Active Management Area, Santa Cruz and Pima Counties, Arizona. Arizona Department of Water Resources Modeling Report No. 18.

Dominguez, F., Cañon, J., Valdes, J., 2010. IPCC-AR4 climate simulations for the southwestern U.S.: the importance of future ENSO projections. Clim. Change 99, 499–514. http://dx.doi.org/10.1007/s10584-009-9672-5.

Erwin, G., 2007. Groundwater Flow Model of the Santa Cruz Active Management Area Microbasins International Boundary to Nogales International Wastewater Treatment Plant Santa Cruz County. Arizona Department of Water Resources, Modeling Report #15.

Garfin, G., Jardine, A., Merideth, R., Black, M., LeRoy, S. (Eds.), 2013. Assessment of Climate Change in the Southwest United States: A Report Prepared for the National Climate Assessment. A Report by the Southwest Climate Alliance. Island Press, Washington, DC.

Geil, K.L., Serra, Y.L., Zeng, X., 2013. Assessment of the CMIP5 model simulations of the North American Monsoon system. J. Clim. 26, 8787–8801.

Georgakakos, A.P., Yao, H., Kistenmacher, M., Georgakakos, K.P., Graham, N.E., Cheng, F.Y., Spencer, C., Shamir, E., 2012. Value of adaptive water resources management in Northern California under climatic variability and change: reservoir management. J. Hydrol. 412, 34–46. http://dx.doi.org/10.1016/j.jhydrol.2011.04.038.

Grantz, K., Rajagopalan, M., Clark, M., Zagona, E., 2007. Seasonal shifts in the North American monsoon. J. Clim. 20 (9), 1923–1935.

Halpenny, L.C., Halpenny, P.C., 1988. Review of the Hydrogeology of the Santa Cruz Basin in the Vicinity of the Santa Cruz-Pima County Line: Tucson, Arizona. Water Development Corporation, 59p.

Hirschboeck, K.K., 1985. Hydroclimatology of Flow Events in the Gila River Basin, Central and Southern Arizona. Ph.D. Dissertation, University of Arizona, Tucson.

Lite, S.J., Stromberg, J.C., 2005. Surface water and groundwater thresholds for maintaining Populus-Salix forests, San Pedro River, Arizona. Biol. Conserv. 125, 153–167.

Liu, Y., Sun, A.Y., Nelson, K., Hipke, W.E., 2012. Cloud computing for integrated stochastic groundwater uncertainty analysis. Int. J. Digit. Earth 2012, 1–25.

Maurer, E.P., Wood, A.W., Adam, J.C., Lettenmaier, D.P., Nijssen, B., 2002. A long-term hydrologically-based data set of land surface fluxes and states for the conterminous United States. J. Clim. 15 (22), 3237–3251.

Maurer, E.P., Brekke, L.D., Pruitt, T., Duffy, P.B., 2007. Fine-resolution climate change projections enhance regional climate change impact studies. Eos Trans. Am. Geophys. Union 88, 504. http://dx.doi.org/10.1029/2007EO470006.

Mearns, L.O. et al., 2007. The North American Regional Climate Change Assessment Program Dataset. National Center for Atmospheric Research Earth System Grid Data Portal, Boulder, CO, http://dx.doi.org/10.5065/D6RN35ST (downloaded 18.09.13) (updated 2011).

Morin, E., Goodrich, D.C., Maddox, R.A., Gao, X., Gupta, H.V., Sorooshian, S., 2005. Spatial patterns in thunderstorm rainfall events and their coupling with watershed hydrological response. Adv. Water Resour. 29 (6), 843–860.

Nadeau, J., Megdal, S.B., 2012. Arizona Environmental Water Needs Assessment Report. University of Arizona Water Resources Research Center (Reprint).

Nelson, K., 2007. Groundwater Flow Model of the Santa Cruz Active Management Area along the Effluent-Dominated Santa Cruz River, Santa Cruz and Pima Counties, Arizona. Arizona Department of Water Resources, Modeling Report No. 14.

Nelson, K., 2010. Risk Assessment of Pumping Impacts on Simulated Groundwater Flow in the Santa Cruz Active Management Area. ADWR Modeling Report No. 21, May 2010.

Paschalis, A., Molnar, P., Fatichi, S., Burlando, P., 2013. A stochastic model for high-resolution space-time precipitation simulation. Water Resour. Res. 49, 8400–8417. http://dx.doi.org/10.1002/2013wr014437.

Peleg, N., Morin, E., 2014. Stochastic convective rain-field simulation using a high-resolution synoptically conditioned weather generator (HiReS-WG). Water Resour. Res. 50, 2124–2139. http://dx.doi.org/10.1002/2013wr014836.

Peleg, N., Shamir, E., Georgakakos, K.P., Morin, E., 2014. A framework for assessing hydrological regime sensitivity to climate change in a convective rainfall environment: a case study of two medium-sized eastern Mediterranean catchments, Israel. Hessd 11, 10553–10592.

Randel, D.A. et al., 2007. Climate models and their evaluation. In: Solomon et al. (Eds.), Climate Change 2007: The Physical Basis. Cambridge University Press, Cambridge, pp. 589–662.

Reclamation, 2011. West-Wide Climate Risk Assessments: Bias-Corrected and Spatially Downscaled Surface Water Projections'. Technical Memorandum No. 86-68210-2011-01. U.S. Department of the Interior, Bureau of Reclamation, Technical Services Center, Denver, Colorado, 138 pp.

Seth, A., Rauscher, S.A., Rojas, M., Giannini, A., Camargo, S.J., 2011. Enhanced spring convective barrier for monsoons in warmer worlds? Clim. Change 104 (2), 403–414.

Shafroth, P.B., Auble, G.T., Stromberg, J.C., Patten, D.T., 1998. Establishment of woody riparian vegetation in relation to annual patterns of streamflow, Bill Williams River, Arizona. Wetlands 18, 577–590.

Shamir, E., 2014. Modification and Calibration of the Hydrologic Modeling Framework for the Santa Cruz River Basin, Arizona. HRC Technical Note No. 71. Hydrologic Research Center, San Diego, CA, <http://www.hrc-lab.org/projects/projectpdfs/HRCTN71_20140901.pdf> (01.09.14).

Shamir, E., Graham, N.E., Wang, J., Meko, D.M., Georgakakos, K.P., 2005. Stochastic Streamflow Scenarios for the Santa-Cruz River at the Nogales Gauge. Hydrologic Research Center Technical Report No. 4. Arizona Department of Water Resources, Santa Cruz, AMA, <http://www.hrc-lab.org/projects/dsp_projectSubPage.php?subpage=santacruz> (December 2005).

Shamir, E., Wang, J., Georgakakos, K.P., 2007a. Probabilistic streamflow generation model for data sparse arid watersheds. J. Am. Water Resour. Assoc. 43 (5), 1142–1154.

Shamir, E., Graham, N.E., Meko, D.M., Georgakakos, K.P., 2007b. Hydrologic model for water resources planning in Santa-Cruz River, Southern Arizona. J. Am. Water Resour. Assoc. 43 (5), 1155–1170.

Shamir, E., Carrillo, C., Castro, L.C., Chang, H.-I., Megdal, S., Eden, S., Prietto, J., 2014. Water resources vulnerability to climate change in the Upper Santa Cruz River, Arizona. In: Ames, Daniel P., Quinn, Nigel W.T., Rizzoli, Andrea E. (Eds.), 7th Intl. Congress on Env. Modelling and Software, International Environmental Modelling and Software Society (iEMSs), San Diego, CA, USA. <http://www.iemss.org/society/index.php/iemss-2014-proceedings>.

Snyder, D.L., Miller, M.I., 1997. Random Point Processes in Time and Space. Springer, New York.

Snyder, K.A., Williams, G., 2000. Water resources used by riparian trees varies among stream types on the San Pedro River, Arizona. Agric. For. Meteorol. 105, 227–240.

Stromberg, J., Lite, S.J., Dixon, M.D., Tiller, R., 2009. Status of the Upper San Pedro (USA): riparian ecosystem. In: Stromberg, J.C., Tellman, B.J. (Eds.), Ecology and Conservation of the San Pedro River. University of Arizona Press, Tucson, AZ.

Stromberg, J.C., McCluney, K.E., Dixon, M.D., Meixner, T., 2012. Dryland riparian ecosystems in the American Southwest: sensitivity and resilience to climatic extremes. Ecosystems. http://dx.doi.org/10.1007/s10021-012-9603-3.

Thomas, B., Pool, D.R., 2006. Seasonal Precipitation and Streamflow Trends in Southeastern Arizona and Southwestern New Mexico. U.S. Geological Survey Professional Paper 2005-1712, 79 pp.

Wilby, R.L., Wigley, T.M.L., 1997. Downscaling general circulation model output: a review of methods and limitations. Prog. Phys. Geogr. 21, 530–548. http://dx.doi.org/10.1177/030913339702100403.

Wilks, D.S., Wilby, R.L., 1999. The weather generation game: a review of stochastic weather models. Prog. Phys. Geogr. 23, 329–357. http://dx.doi.org/10.1177/030913339902300302.

Zhang, Y., Qian, Y., Dulière, V., Salathé, E.P., Leung, L.R., 2012. ENSO anomalies over the western United States: present and future patterns in regional climate model simulations. Clim. Change 110, 315–346. http://dx.doi.org/10.1007/s10584-011-0088-7.